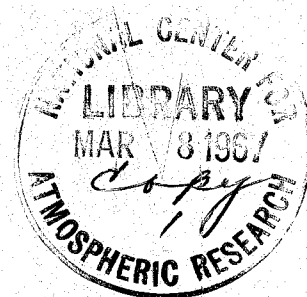


02061

NCAR-TN-25



# Balloon Shapes and Stresses Below the Design Altitude

JUSTIN H. SMALLEY

December 1966

---

**NCAR Technical Notes**

NATIONAL CENTER FOR ATMOSPHERIC RESEARCH  
Boulder, Colorado

0-2061

NCAR LIBRARY

NCAR Library



5 0583 01004590 8

The National Center for Atmospheric Research (NCAR) is dedicated to the advancement of the atmospheric sciences for the benefit of mankind. It is operated by the University Corporation for Atmospheric Research (UCAR), a private, university-controlled, non-profit organization, and is sponsored and principally funded by the National Science Foundation.

NCAR shares with other atmospheric research groups four inter-related, long-range objectives that provide justification for major expenditures of public and private funds:

- To ascertain the feasibility of controlling weather and climate, to develop the techniques for control, and to bring about the beneficial application of this knowledge;
- To bring about improved description and prediction of astrophysical influences on the atmosphere and the space environment of our planet;
- To bring about improved description and prediction of atmospheric processes and the forecasting of weather and climate;
- To improve our understanding of the sources of air contamination and to bring about the application of better practices of air conservation.

The research and facilities operations of NCAR are conducted in four organizational entities:

The Laboratory of Atmospheric Sciences

The High Altitude Observatory

The Facilities Laboratory

The Advanced Study Program

All visiting scientist programs and joint-use facilities of NCAR are available to scientists from UCAR-member and non-member institutions (including private and government laboratories in the United States and abroad) on an equal basis. The member universities of UCAR are:

University of Alaska	Florida State University	University of Oklahoma
University of Arizona	University of Hawaii	Pennsylvania State University
University of California	The Johns Hopkins University	Saint Louis University
University of Chicago	Massachusetts Institute of Technology	Texas A & M University
Colorado State University	University of Michigan	University of Texas
University of Colorado	University of Minnesota	University of Utah
Cornell University	New York University	University of Washington
University of Denver		University of Wisconsin

NCAR-TN-25

# **Balloon Shapes and Stresses Below the Design Altitude**

JUSTIN H. SMALLEY

December 1966



### PREFACE

The design data for natural-shape balloons, published in 1952, have been used to design thousands of balloons. These data, however, describe the balloon only at its float altitude. Most balloon failures occur during ascent, indicating that stress on the balloon is greater than under float conditions. The present study provides some of the information needed to understand the stresses in ascending balloons.

### SUMMARY

Shapes and stresses were calculated for natural-shape balloons, in equilibrium, at altitudes below their design altitude. The balloon material was assumed to be symmetrically deployed about the vertical axis, and the balloons were assumed to have zero pressure at the bottom apex when at their design altitude.

Results are presented for balloons assumed to be weightless; these results are independent of style or design. Results are also presented for three fully tailored balloons with material weight corresponding to  $\Sigma = 0.2$ ,  $0.4$ , and  $1.0$ , and for two full-cylinder balloons with  $\Sigma = 0.422$  and  $0.924$ . These two types represent the extremes of possible designs.

When the zero pressure level is measured in terms of gore length (reducing the effect of balloon size), the changes due to style of design are quite small. A single curve will suffice for many purposes.



CONTENTS

Preface . . . . .	iii
Summary . . . . .	iii
List of Tables. . . . .	vii
List of Figures . . . . .	ix
List of Symbols . . . . .	xi
INTRODUCTION. . . . .	1
ANALYSIS. . . . .	1
RESULTS . . . . .	2
DISCUSSION. . . . .	3
References. . . . .	4
Tables. . . . .	5
Figures . . . . .	11





TABLES

1.	A balloon below its design altitude, $\Sigma = 0$ , all configurations . . . . .	5
2.	A balloon below its design altitude, $\Sigma = 0.2$ , fully tailored . . . . .	6
3.	A balloon below its design altitude, $\Sigma = 0.4$ , fully tailored . . . . .	7
4.	A balloon below its design altitude, $\Sigma = 1.0$ , fully tailored . . . . .	8
5.	A balloon below its design altitude, $\Sigma = 0.422$ , cylinder . . . . .	9
6.	A balloon below its design altitude, $\Sigma = 0.924$ , cylinder . . . . .	10



FIGURES

1. Shapes of a fully tailored balloon below its design altitude, $\Sigma = 0$ . . . . .	11
2. Shapes of a fully tailored balloon below its design altitude, $\Sigma = 0.2$ . . . . .	12
3. Shapes of a fully tailored balloon below its design altitude, $\Sigma = 0.4$ . . . . .	13
4. Shapes of a fully tailored balloon below its design altitude, $\Sigma = 1.0$ . . . . .	14
5. Pressure at the top of a fully tailored, natural-shape balloon . . . . .	15
6. Pressure head at the top of a fully tailored, natural-shape balloon and a sphere. . . . .	16
7. Height of zero-pressure level in a balloon below its design altitude, in $\lambda$ units . . . . .	17
8. Height of zero-pressure level in a balloon below its design altitude, in gore length units . . . . .	18
9. Relative meridional stress at the top and bottom of a balloon which is below its design altitude. . . . .	19



SYMBOLS

a	Position of zero-pressure level above bottom of balloon (length)
b	Unit lift of inflation gas (force per unit volume)
d	Subscript denoting conditions at the design altitude
G	Gross lift of balloon (force), $G/P = (V/\lambda^3)_d$
P	Payload of balloon (force)
p	Gas Pressure at top of balloon (force per unit area)
r	Radius coordinate of balloon, measured from the vertical axis of symmetry (length)
S	Total gore length of balloon (length)
V	Volume of balloon (length cubed)
z	Height coordinate of balloon, measured upwards from the bottom apex (length)
$\lambda$	Characteristic length (length), $\lambda^3 = P/b$
$\alpha$	$a/\lambda$



## INTRODUCTION

The shapes and stresses of balloons at their design altitude (i.e., float altitude) have been known for some time (Refs. 1 and 2). Equally of interest, however, are the shapes and stresses of balloons as they ascend to their design altitude. As a first step, these factors have been determined assuming rotational symmetry. Because balloons are not rotationally symmetrical the stress data are of secondary value, but the pressure information is particularly useful to designers of tandem systems and to investigators of the deployment of the ascending balloon.

## ANALYSIS

The equations used to determine the shape are the same as those in Ref. 2. Integration was performed on the NCAR Control Data 6600 computer. It was assumed that the balloon was lifting a fixed payload,\* that is, its design payload. The problem was handled as a "quasi-steady" case by assuming that for a particular set of conditions the balloon was at a constant altitude. Calculations were then carried out for a given value of subpressure, with the initial conditions being adjusted until a shape was found with a flat top and with the proper gore length. The subpressure was varied until the resultant volume was just sufficient to lift the payload and the balloon.

At low altitudes the majority of the balloon material hangs as a rope of dead weight. Because the solution of the equations is sensitive to the initial angle, it was not practical to consider this rope of material by starting with an exceedingly small initial angle.

---

\* In the interests of generality, consideration of free lift has been omitted. It could easily be included when studying a specific case.

Accordingly, integration of the equations started at a point upwards along the gore where the initial angle would be about one-half of one degree; the weight of material below that point was added to the payload. The weight distribution of material in the balloon was predetermined from the weight distribution of the fully inflated balloon.

### RESULTS

Starting with design data for four fully tailored and two cylinder natural-shape balloons with all the payload at the bottom apex, the shape, stresses, zero-pressure level and top pressure have been determined at ten altitudes below the design altitude. Rather than use specific altitudes, the results have been made more general by finding the above values at altitudes where the unit lift is certain multiples of the unit lift at the design altitude. The results are presented in tables 1 through 6. It should be noted that the values are given in terms of gore length.

The gore position and the radius at the zero-pressure level are listed as being approximate values. One hundred gore positions are given in the printed output from the computer. In the tables the gore length and radius values listed are those points from the computer output with a height most nearly corresponding to that of the zero-pressure level; it was felt that it would not be productive to take the necessary steps to find more accurate gore length and radius values. The points given for the maximum radius are, again, the nearest values from the printed computer output.

The shapes for the fully tailored balloons have been sketched in Figs. 1 through 4. In these figures all shapes have been drawn with the position of the bottom apex at a common point.

In Fig. 5 the pressure in the top of the fully tailored balloon has been presented in terms of  $\lambda$ . The same data are presented in Fig. 6 in terms of gore length. The height of the zero-pressure



level in both  $\lambda$  units and gore length units is shown in Figs. 7 and 8 respectively. Examples of the resulting meridional stresses are given in Fig. 9.

### DISCUSSION

On each shape the zero-pressure level has been indicated. Note that for real balloons with finite material weight, the zero-pressure level is above the inflection point (Figs. 2, 3 and 4). The "hook" in the pressure curves of Fig. 5 is most interesting: it is explained by the fact that as the balloon approaches float (as  $b/b_d$  approaches 1.0), the part of the balloon filling with the expanding gas is conical whereas, at lower altitudes, the part filling is more nearly spherical. The result is that the zero-pressure level moves downward faster than the unit lift decreases, so that the pressure at the top actually increases.

It has been common practice to assume that the gas bubble was spherical in shape to arrive at an estimate of the zero-pressure level and/or an estimate of the gas pressure in the top of the balloon; the diameter was used as the pressure head. With the data presented herein this assumption will no longer be necessary. In Fig. 6 a comparison is made of the present results with this spherical shape assumption: it is seen that the assumption yields a conservative estimate for the pressure.

The volume of the balloon at the various altitudes has not been given but is easily determined. In  $\lambda$  units it is

$$\frac{V}{\lambda_d^3} = \left( \frac{G}{P} \right) \div \left( \frac{b}{b_d} \right) .$$

This may be converted to gore length units with the relation

$$\frac{V}{S^3} = \left( \frac{V}{\lambda_d^3} \right) \div \left( \frac{S}{\lambda_d} \right)^3 .$$

The necessary G/P and  $S/\lambda_d$  values for each balloon are included in the tables.

#### REFERENCES

1. University of Minnesota, Department of Physics: "Research and Development in the Field of High Altitude Plastic Balloons," Contract Nonr-710(01), Vol. 1-2, 13 December 1951 to 15 June 1952.
2. Smalley, J. H.: "Determination of the Shape of a Free Balloon: Theoretical Development," General Mills, Inc., Electronics Division, Report 2421, Contract AF 19(628)-2783, 2 August 1963.
3. Smalley, J. H.: "Free Balloons with Off-Design Payloads," Litton Systems, Inc., Applied Science Division, Report No. 2927, Contract AF 19(628)5131, 31 December 1965.

TABLE 1

A Balloon Below Its Design Altitude,  $\Sigma = 0$ , All Configurations

	Bottom of Bubble		Zero Pressure Level			At Maximum Radius		
$b/b_d$	Gore Position	Initial Angle**	Gore Position*	Radius*	Height	Radius*	Height*	Balloon Height
1.0	0	50.15	0	0	0	0.3270	0.422	0.6439
1.1	0	41.86	0.16	0.108	0.1163	0.3116	0.463	0.6769
1.2	0	35.76	0.23	0.139	0.1859	0.2994	0.498	0.7000
1.5	0	23.92	0.34	0.163	0.2993	0.2730	0.551	0.7421
2.5	0	8.33	0.47	0.150	0.4399	0.2268	0.634	0.7969
6	0	0.50	0.61	0.114	0.5850	0.1690	0.737	0.8502
15	0.25	0.39	0.71	0.083	0.6942	0.1245	0.806	0.8896
40	0.50	1.03	0.79	0.059	0.7795	0.0897	0.857	0.9204
100	0.62	0.72	0.85	0.046	0.8375	0.0661	0.897	0.9413
300	0.73	0.53	0.89	0.029	0.8873	0.0457	0.931	0.9593
1000	0.80	0.13	0.93	0.021	0.9246	0.0306	0.954	0.9728

$$S/\lambda_d = 1.99441$$

$$G/P = 1.00000$$

\* Approximate values

\*\* Angle in degrees

TABLE 2

A Balloon Below Its Design Altitude,  $\Sigma = 0.2$ , Fully Tailored

	Bottom of Bubble		Zero Pressure Level			At Maximum Radius		
b/b d	Gore Position	Initial Angle**	Gore Position*	Radius*	Height	Radius*	Height*	Balloon Height
1.0	0	58.89	0	0	0	0.3460	0.371	0.5985
1.1	0	47.14	0.20	0.148	0.1368	0.3289	0.428	0.6428
1.2	0	39.13	0.27	0.179	0.2054	0.3158	0.461	0.6709
1.5	0	24.50	0.37	0.195	0.3093	0.2878	0.529	0.7191
2.5	0	7.16	0.48	0.169	0.4381	0.2384	0.615	0.7802
6	0	0.26	0.60	0.119	0.5796	0.1760	0.718	0.8411
15	0.26	0.37	0.71	0.090	0.6884	0.1289	0.794	0.8846
40	0.45	0.33	0.79	0.064	0.7743	0.0927	0.852	0.9174
100	0.57	0.16	0.84	0.045	0.8333	0.0680	0.892	0.9394
300	0.70	0.17	0.89	0.031	0.8842	0.0470	0.925	0.9581
1000	0.80	0.19	0.93	0.023	0.9224	0.0313	0.950	0.9720

$$S/\lambda_d = 2.35043$$

$$G/P = 1.78385$$

\* Approximate values

\*\* Angle in degrees

TABLE 3

A Balloon Below Its Design Altitude,  $\Sigma = 0.4$ , Fully Tailored

	Bottom of Bubble		Zero Pressure Level			At Maximum Radius		
$b/b_d$	Gore Position	Initial Angle**	Gore Position*	Radius*	Height	Radius*	Height*	Balloon Height
1.0	0	67.92	0	0	0	0.3609	0.328	0.5543
1.1	0	50.94	0.26	0.205	0.1636	0.3422	0.393	0.6137
1.2	0	40.62	0.32	0.226	0.2265	0.3286	0.436	0.6462
1.5	0	23.19	0.39	0.220	0.3177	0.2994	0.498	0.6991
2.5	0	5.28	0.48	0.179	0.4366	0.2468	0.598	0.7663
6	0	0.10	0.60	0.126	0.5760	0.1808	0.710	0.8345
15	0.26	0.29	0.70	0.089	0.6845	0.1319	0.792	0.8812
40	0.45	0.33	0.78	0.062	0.7708	0.0946	0.851	0.9154
100	0.57	0.18	0.84	0.047	0.8304	0.0695	0.886	0.9381
300	0.70	0.21	0.89	0.033	0.8821	0.0481	0.921	0.9572
1000	0.80	0.24	0.93	0.024	0.9210	0.0318	0.954	0.9714

$$s/\lambda_d = 2.87047$$

$$G/P = 3.43819$$

\* Approximate values

\*\* Angle in degrees

TABLE 4

A Balloon Below Its Design Altitude,  $\Sigma = 1.0$ , Fully Tailored

	Bottom of Bubble		Zero Pressure Level			At Maximum Radius		
$b/b_d$	Gore Position	Initial Angle**	Gore Position*	Radius*	Height	Radius*	Height*	Balloon Height
1.0	0	84.28	0	0	0	0.3781	0.247	0.4798
1.1	0	46.78	0.38	0.311	0.2100	0.3587	0.343	0.5711
1.2	0	31.89	0.39	0.293	0.2520	0.3445	0.389	0.6072
1.5	0	12.53	0.43	0.262	0.3235	0.3125	0.466	0.6673
2.5	0	1.03	0.50	0.202	0.4356	0.2548	0.576	0.7489
6	0	0.00	0.61	0.137	0.5740	0.1847	0.706	0.8282
15	0.26	0.16	0.70	0.093	0.6816	0.1342	0.781	0.8783
40	0.45	0.32	0.78	0.065	0.7681	0.0961	0.850	0.9138
100	0.57	0.20	0.84	0.049	0.8282	0.0706	0.886	0.9370
300	0.70	0.24	0.89	0.034	0.8805	0.0489	0.920	0.9565
1000	0.80	0.29	0.92	0.020	0.9198	0.0324	0.944	0.9710

$$S/\lambda_d = 5.31732$$

$$G/P = 22.84669$$

\* Approximate values

\*\* Angle in degrees

TABLE 5

A Balloon Below Its Design Altitude,  $\Sigma = 0.422$ , Cylinder

	Bottom of Bubble		Zero Pressure Level			At Maximum Radius		
$b/b_d$	Gore Position	Initial Angle**	Gore Position*	Radius*	Height	Radius*	Height*	Balloon Height
1.0	0	80.56	0	0	0	0.3725	0.303	0.5044
1.1	0	63.87	0.32	0.255	0.1915	0.3550	0.382	0.5705
1.2	0	52.38	0.36	0.259	0.2469	0.3419	0.427	0.6058
1.5	0	29.86	0.41	0.238	0.3267	0.3125	0.500	0.6639
2.5	0	5.53	0.49	0.189	0.4372	0.2578	0.591	0.7395
6	0	0.05	0.61	0.134	0.5757	0.1881	0.705	0.8182
15	0.270	0.27	0.71	0.097	0.6847	0.1363	0.789	0.8717
40	0.455	0.28	0.785	0.066	0.7710	0.0973	0.844	0.9102
100	0.590	0.28	0.840	0.048	0.8305	0.0712	0.885	0.9350
300	0.700	0.16	0.890	0.034	0.8820	0.0490	0.920	0.9556
1000	0.800	0.21	0.925	0.022	0.9208	0.0327	0.948	0.9706

$$S/\lambda_d = 4.00860$$

$$G/P = 9.59901$$

\* Approximate values

\*\* Angle in degrees

TABLE 6

A Balloon Below Its Design Altitude,  $\Sigma = 0.924$ , Cylinder

	Bottom of Bubble		Zero Pressure Level			At Maximum Radius		
$b/b_d$	Gore Position	Initial Angle**	Gore Position*	Radius*	Height	Radius*	Height*	Balloon Height
1.0	0	88.61	0	0	0	0.3793	0.275	0.4717
1.1	0	81.39	0.36	0.289	0.2109	0.3633	0.370	0.5434
1.2	0	73.44	0.38	0.278	0.2585	0.3498	0.417	0.5831
1.5	0	45.94	0.42	0.250	0.3304	0.3190	0.483	0.6474
2.5	0	5.59	0.49	0.193	0.4371	0.2618	0.586	0.7296
6	0	0.01	0.61	0.136	0.5754	0.1901	0.703	0.8139
15	0.270	0.22	0.71	0.098	0.6842	0.1375	0.778	0.8696
40	0.455	0.26	0.785	0.067	0.7705	0.0980	0.844	0.9091
100	0.590	0.27	0.840	0.049	0.8300	0.0716	0.885	0.9344
300	0.700	0.16	0.890	0.034	0.8816	0.0493	0.920	0.9553
1000	0.800	0.21	0.925	0.022	0.9205	0.0329	0.948	0.9704

$$S/\lambda_d = 8.01457$$

$$G/P = 77.6515$$

\* Approximate values

\*\* Angle in degrees



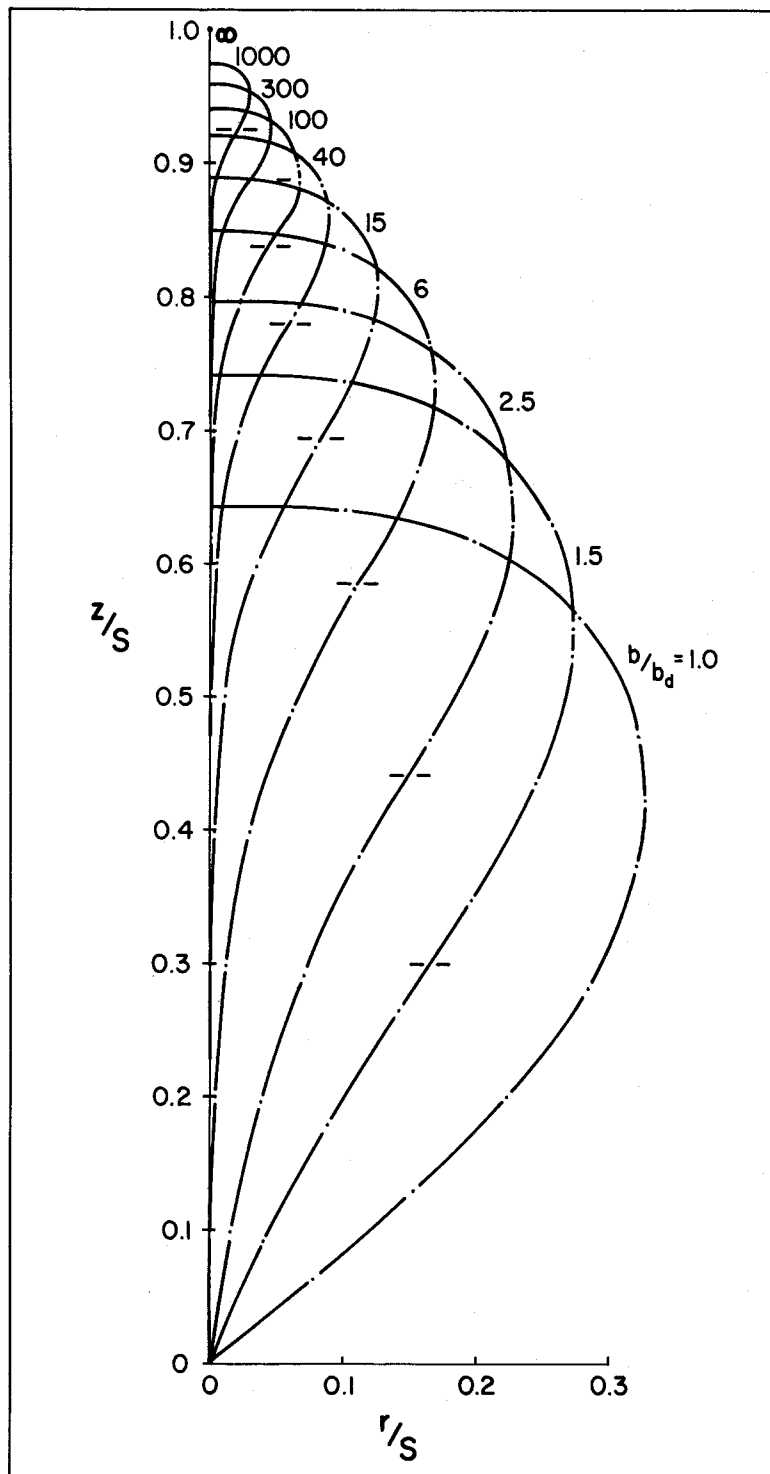


Fig. 1 Shapes of a fully tailored balloon below its design altitude,  $\Sigma = 0$ .

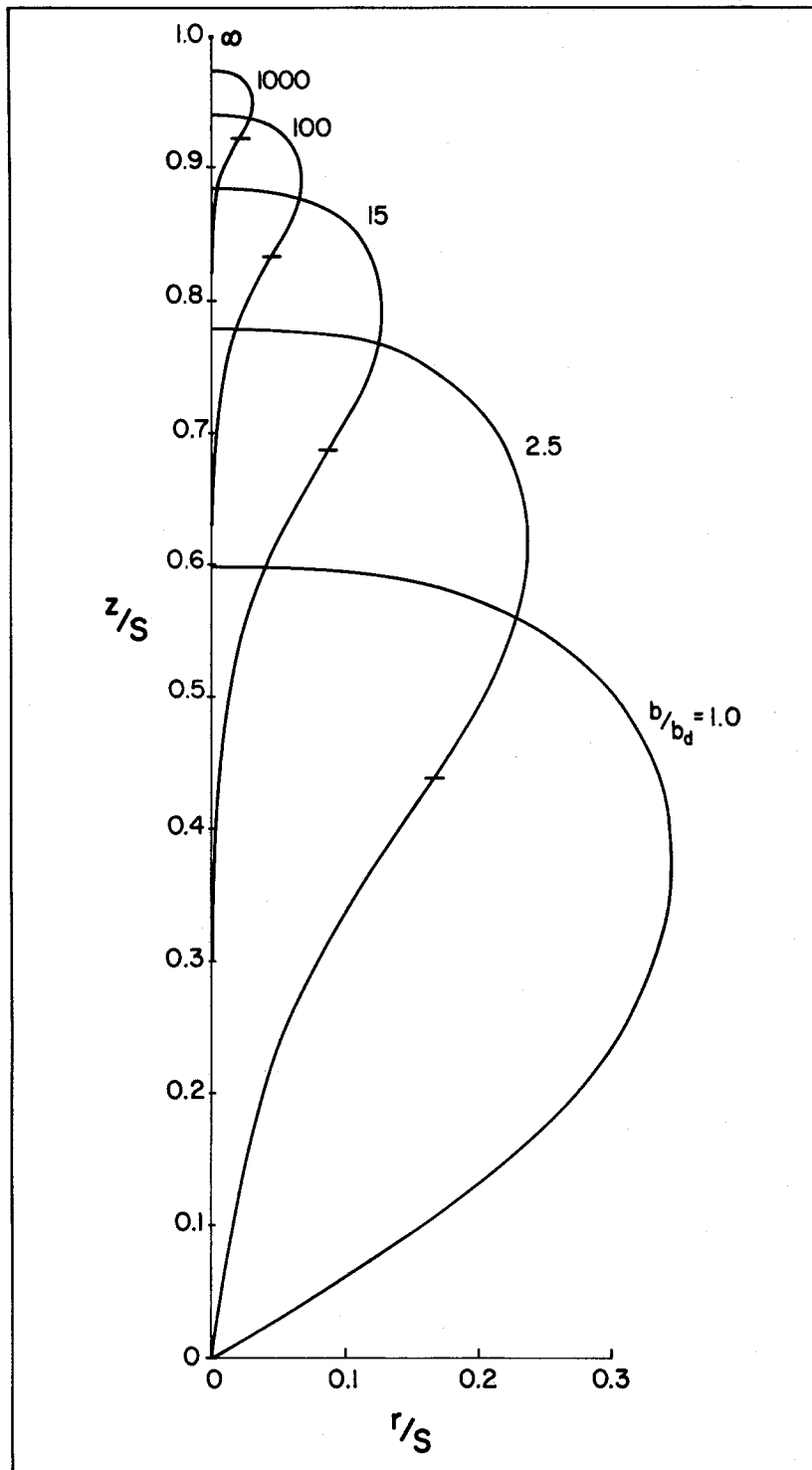


Fig. 2 Shapes of a fully tailored balloon below its design altitude,  $\Sigma = 0.2$ .

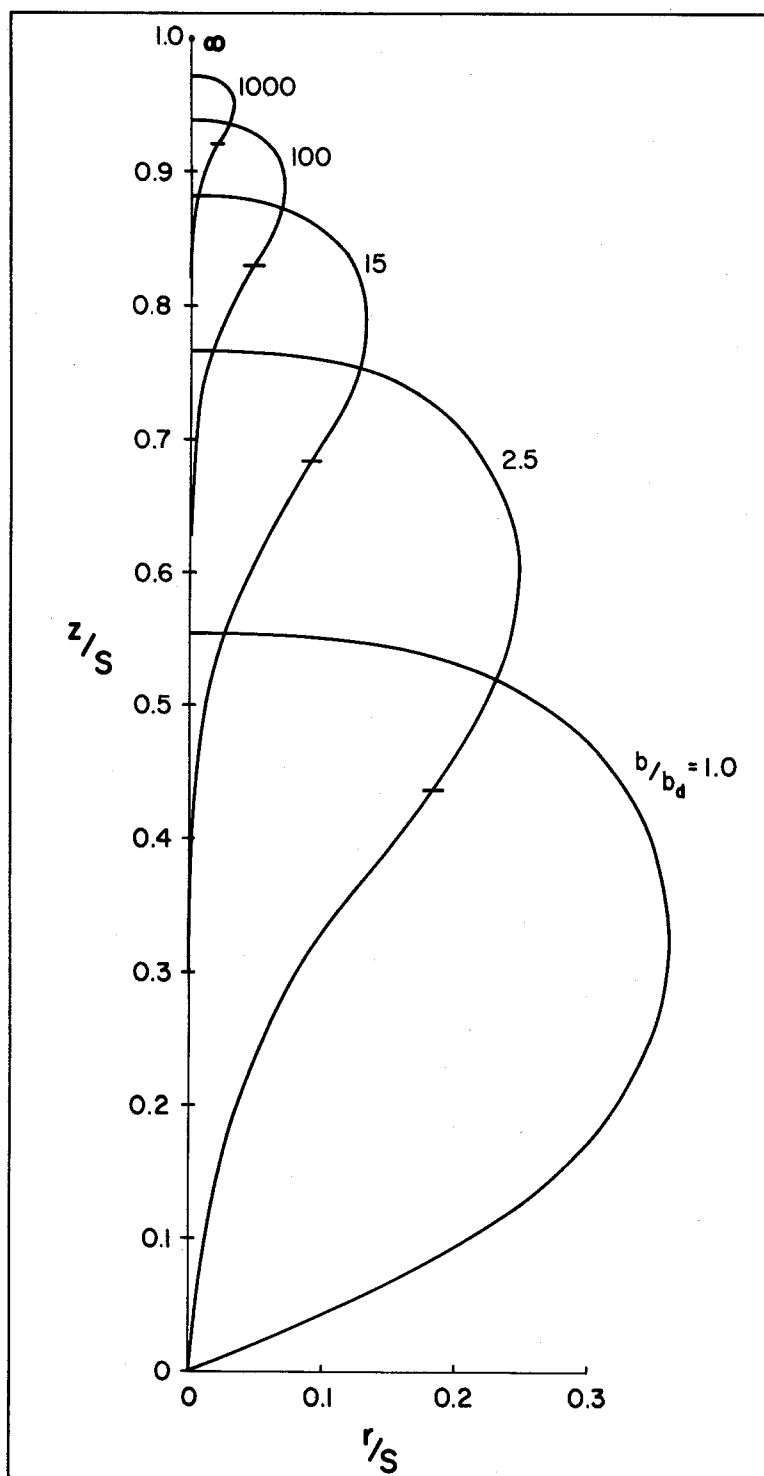


Fig. 3 Shapes of a fully tailored balloon below its design altitude,  $\Sigma = 0.4$ .

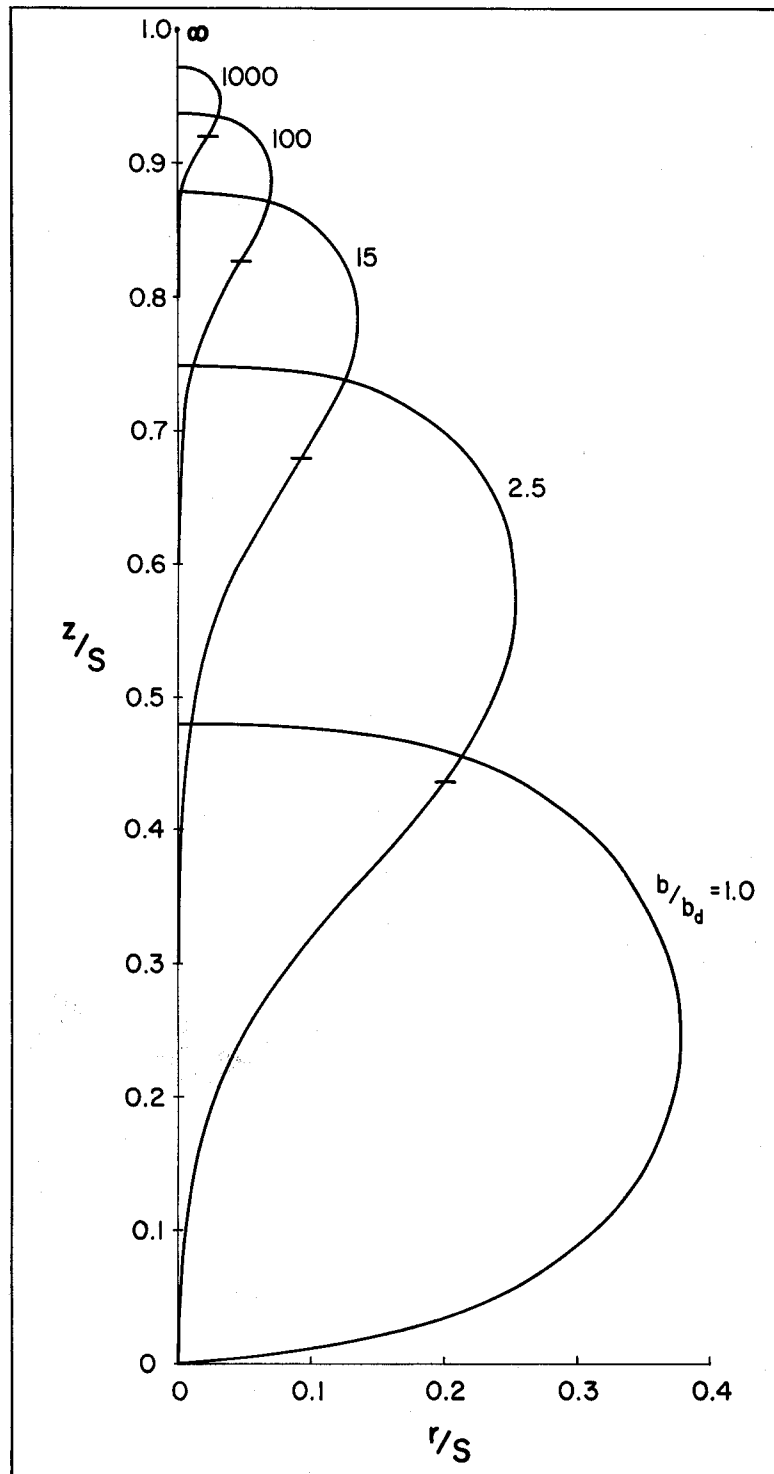


Fig. 4 Shapes of a fully tailored balloon below its design altitude,  $\Sigma = 1.0$ .

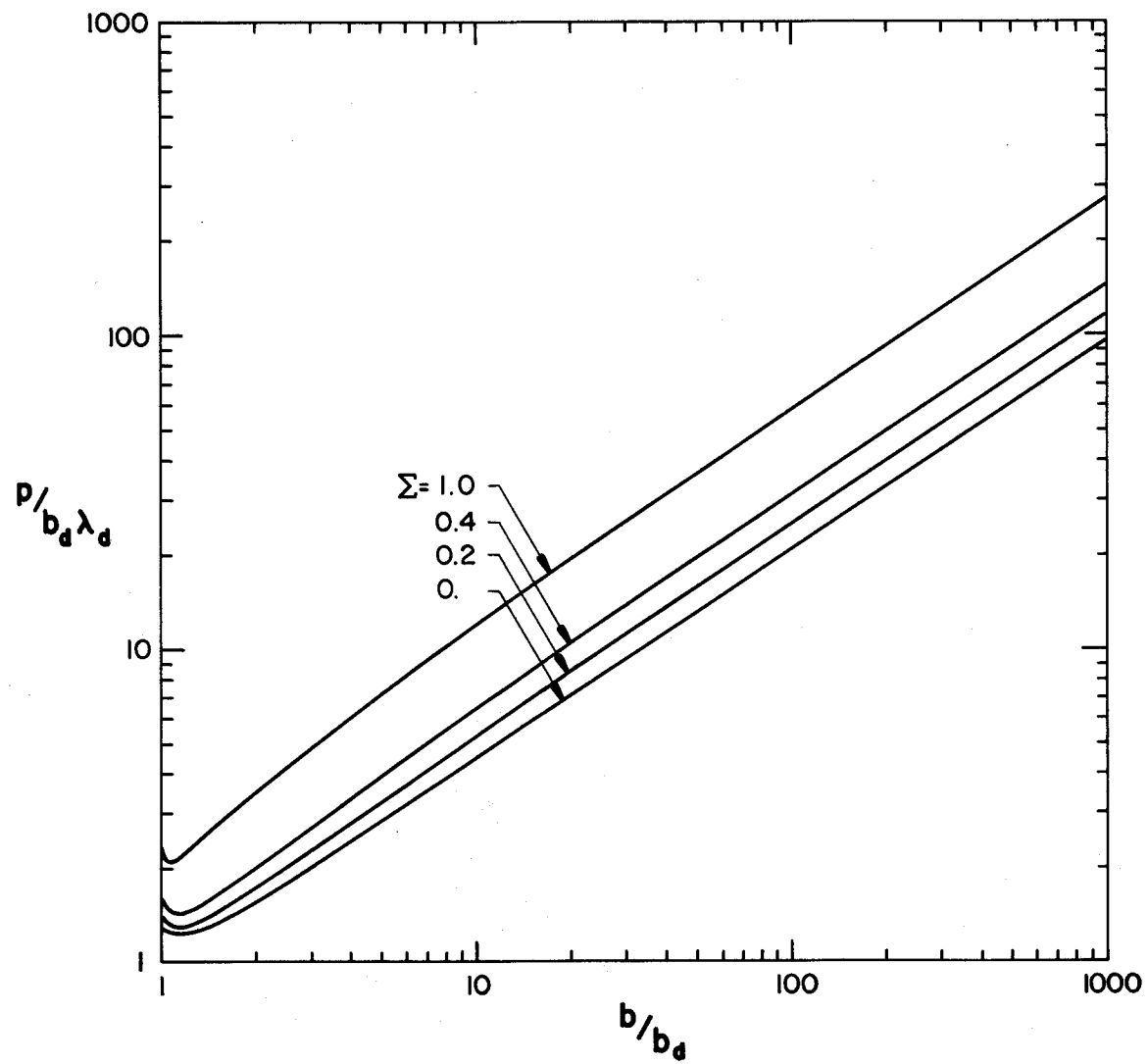


Fig. 5 Pressure at the top of a fully tailored, natural-shape balloon.

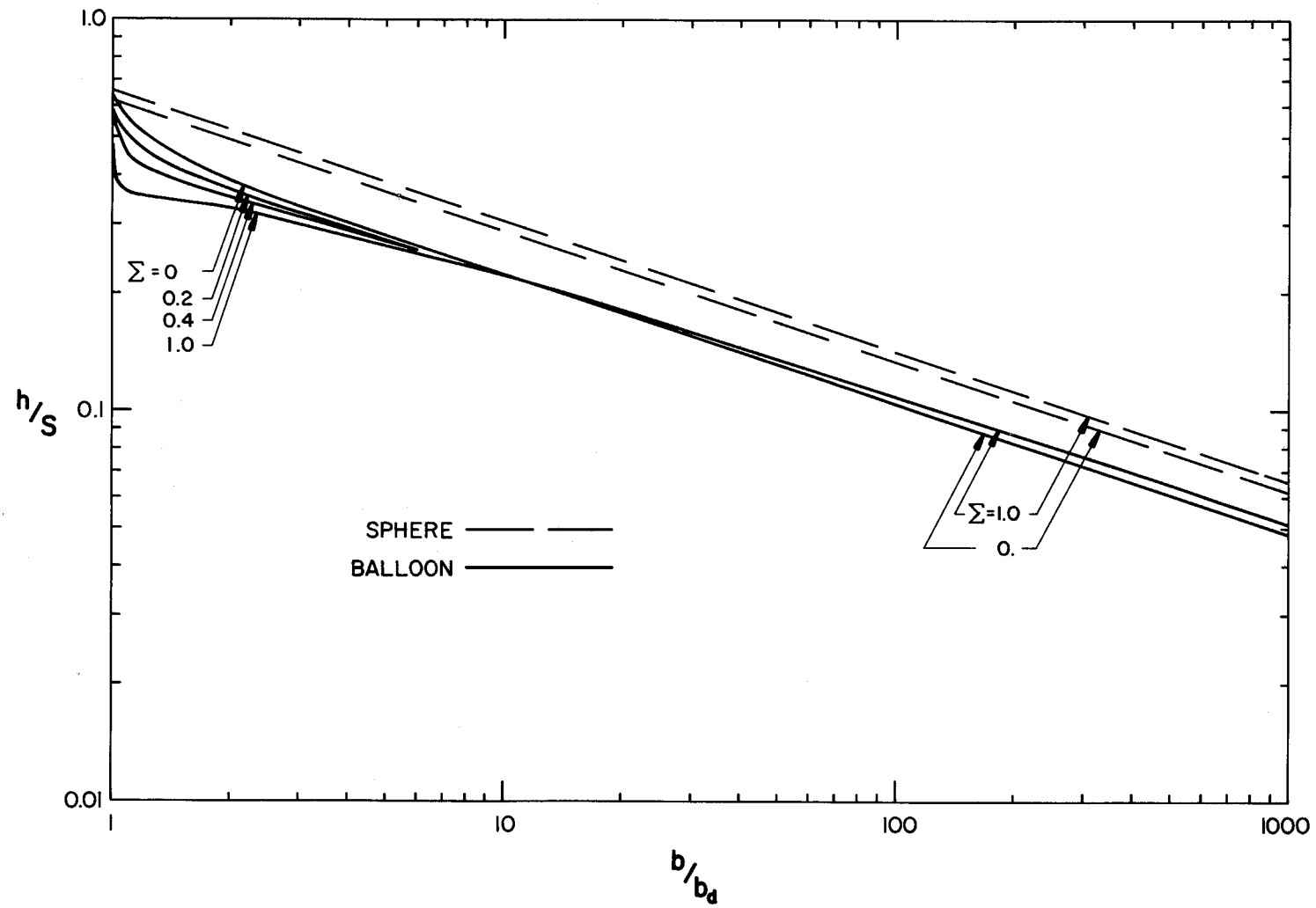


Fig. 6 Pressure head at the top of a fully tailored, natural-shape balloon and a sphere.

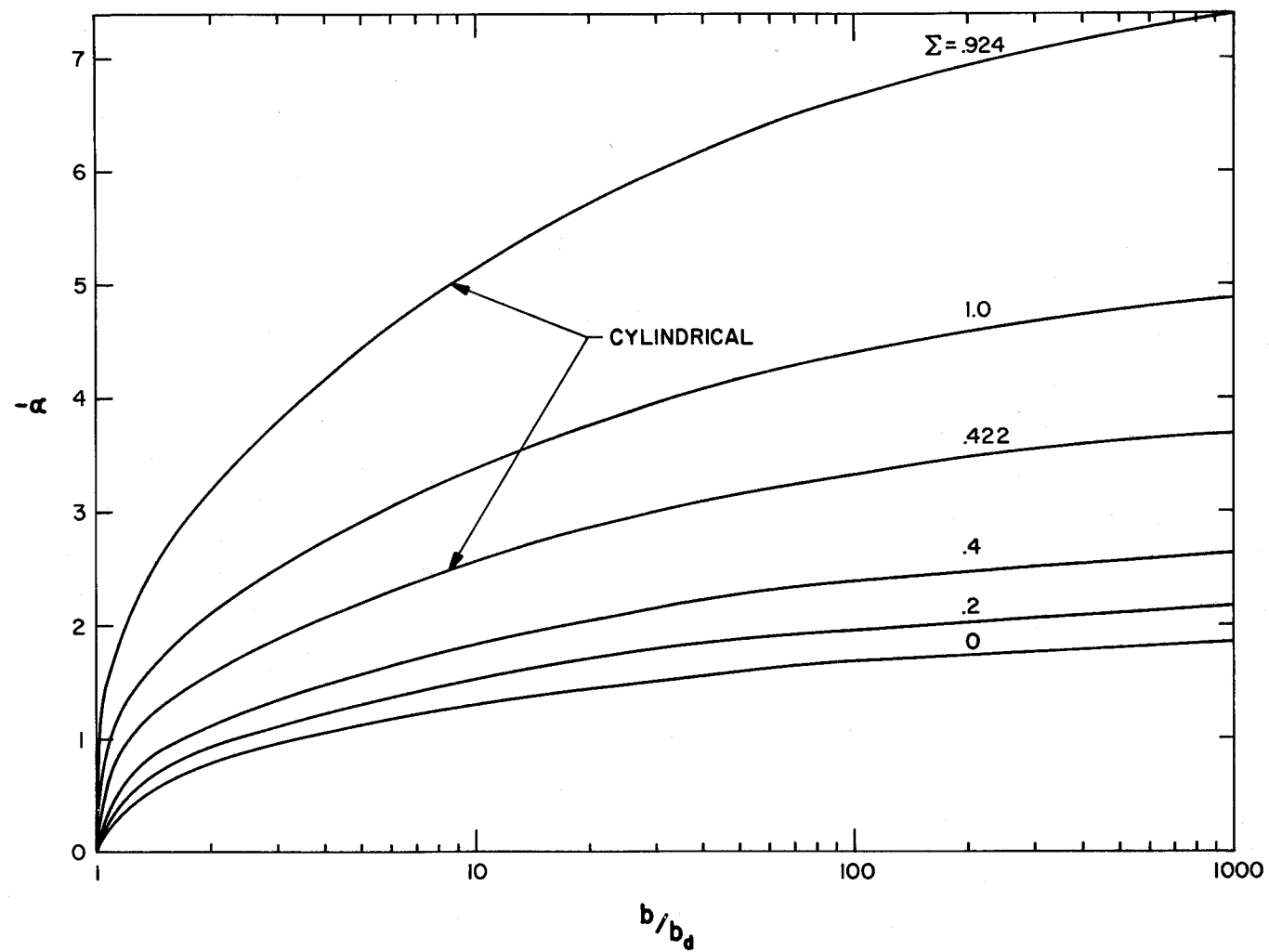


Fig. 7 Height of zero-pressure level in a balloon below its design altitude, in  $\lambda$  units.

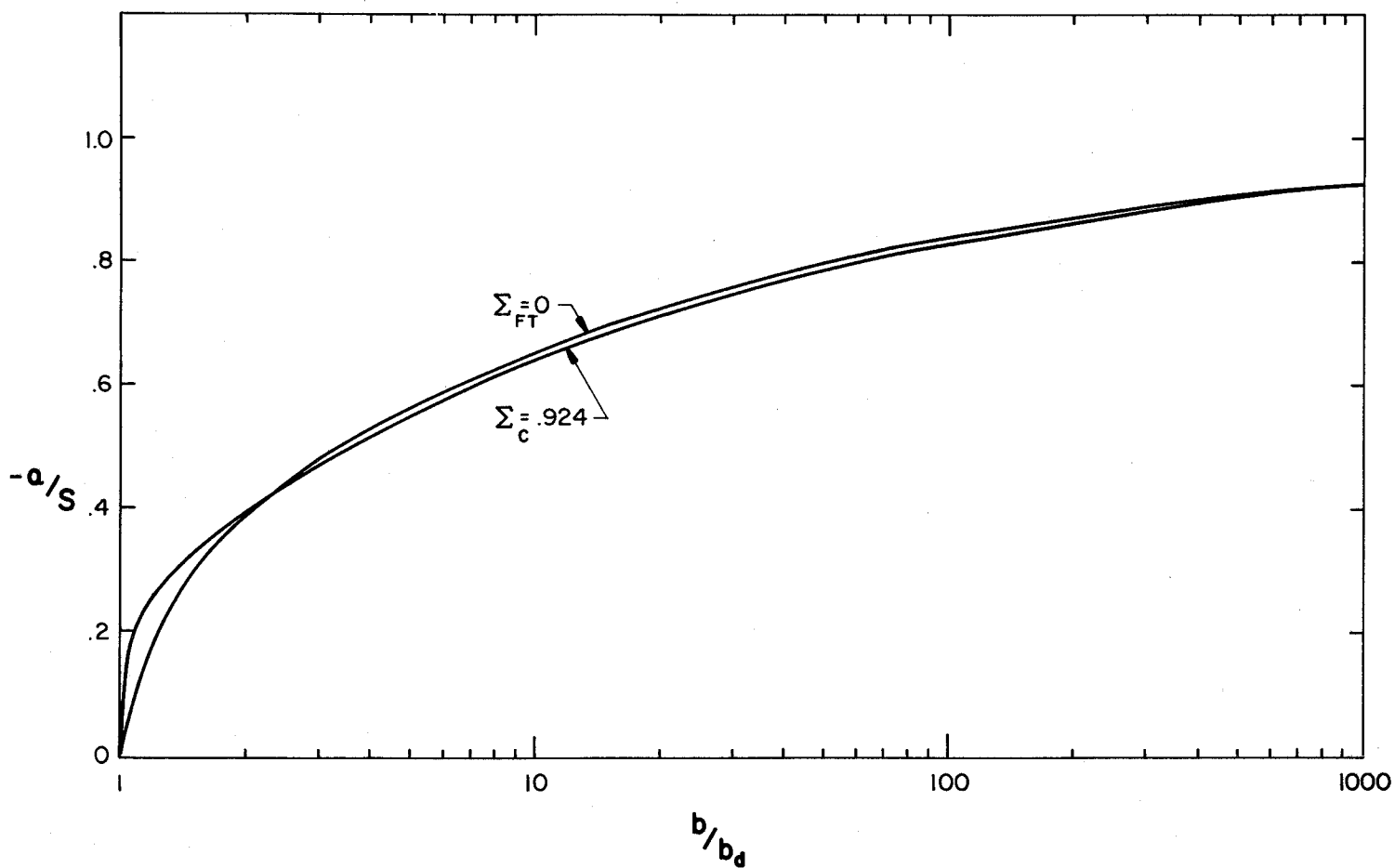


Fig. 8 Height of zero-pressure level in a balloon below its design altitude, in gore length units.



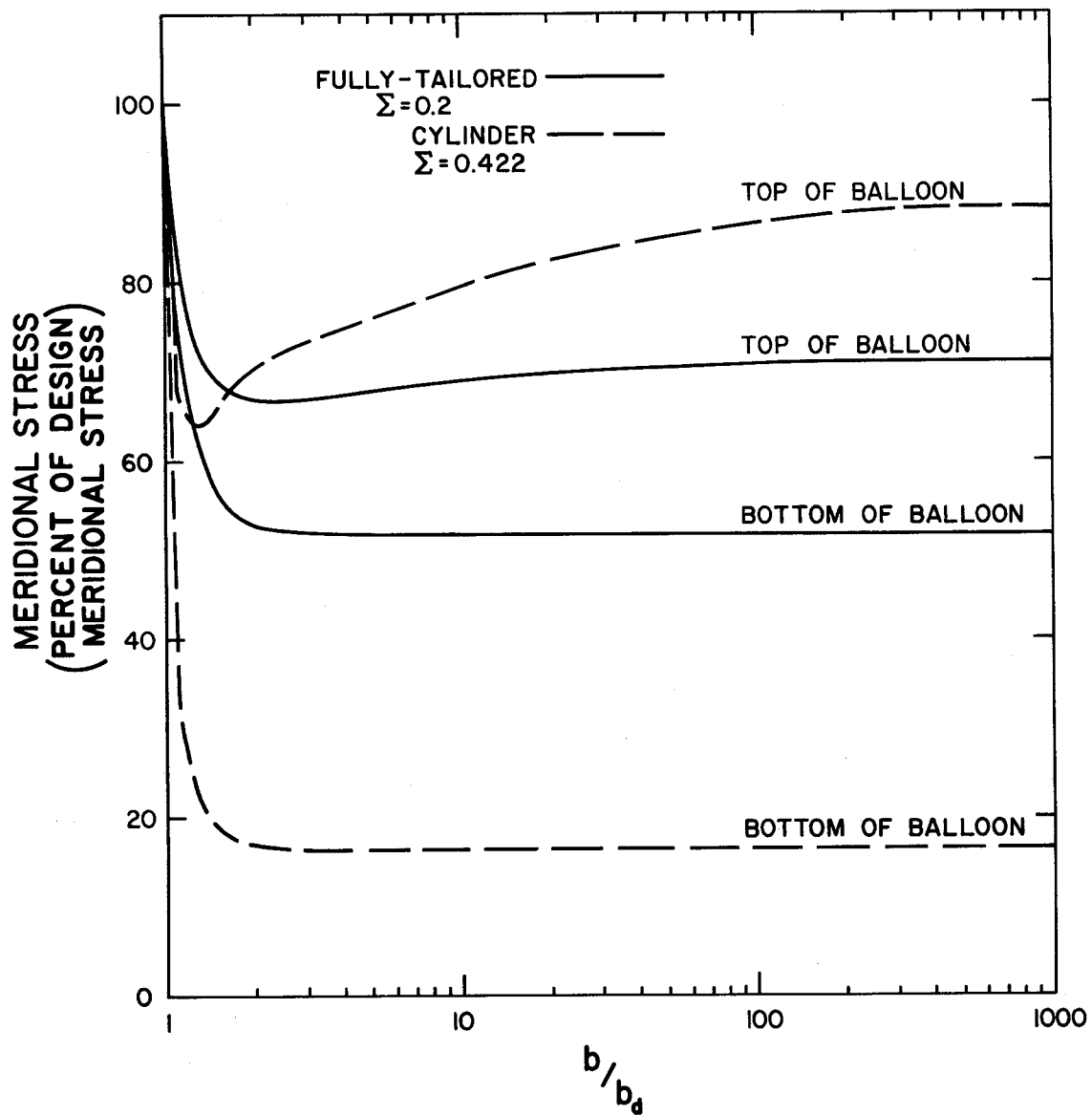


Fig. 9 Relative meridional stress at the top and bottom of a balloon which is below its design altitude.





